Research

Author for correspondence:
Debjani Dutta
e-mail: debs_2000in@yahoo.com;
debjani.dutta@bt.nitdgp.ac.in

Growth profiling, kinetics and substrate utilization of low-cost dairy waste for production of β-cryptoxanthin by *Kocuria marina* DAGII

Ruchira Mitra and Debjani Dutta

Department of Biotechnology, National Institute of Technology Durgapur,
M.G. Avenue, Durgapur 713209, West Bengal, India

iD DD, 0000-0002-2784-3089

The dairy industry produces enormous amount of cheese whey containing the major milk nutrients, but this remains unutilized all over the globe. The present study investigates the production of β-cryptoxanthin (β-CRX) by *Kocuria marina* DAGII using cheese whey as substrate. Response surface methodology (RSM) and an artificial neural network (ANN) approach were implemented to obtain the maximum β-CRX yield. Significant factors, i.e. yeast extract, peptone, cheese whey and initial pH, were the input variables in both the optimizing studies, and β-CRX yield and biomass were taken as output variables. The ANN topology of 4-9-2 was found to be optimum when trained with a feed-forward back-propagation algorithm. Experimental values of β-CRX yield ($17.14\,\mathrm{mg\,l^{-1}}$) and biomass ($5.35\,\mathrm{g\,l^{-1}}$) were compared and ANN predicted values ($16.99\,\mathrm{mg\,l^{-1}}$ and $5.33\,\mathrm{g\,l^{-1}}$, respectively) were found to be more accurate compared with RSM predicted values ($16.95\,\mathrm{mg\,l^{-1}}$ and $5.23\,\mathrm{g\,l^{-1}}$, respectively). Detailed kinetic analysis of cellular growth, substrate consumption and product formation revealed that growth inhibition took place at substrate concentrations higher than 12% (v/v) of cheese whey. The Han and Levenspiel model was the best fitted substrate inhibition model that described the cell growth in cheese whey with an R^2 and MSE of 0.9982% and 0.00477%, respectively. The potential importance of this study lies in the development, optimization and modelling of a suitable cheese whey supplemented medium for increased β-CRX production.

1. Introduction

In recent years, microbial ability to grow on variable substrates has been widely explored for production of different secondary metabolites such as antibiotics, pigments and biosurfactants. The nutritional versatility of microbes makes them highly adaptable and culturable in laboratory conditions. This often leads to novel application of microbes on non-conventional substrates for industrial, pharmaceutical and environmental benefits. In our previous study, the inherent ability of *Kocuria marina* DAGII for production of β-cryptoxanthin (β-CRX) was reported [1]. β-CRX is a mono-oxygenated pro-vitamin A xanthophyll mostly provided by citrus fruits [2]. Administration of β-CRX has revealed various beneficial effects such as anti-oxidant, anti-inflammatory, anti-cancer, anti-obesity and anti-diabetic properties in different *in vitro* and *in vivo* studies [3,4]. β-CRX exerts cardio-protective action and also exhibits a unique regulatory role by maintaining bone health [5,6]. Research on health beneficiary roles of β-CRX is highly progressive, which has promoted development of innovative approaches for β-CRX production. Several methods such as extraction from citrus fruits, chemical transformation of commercial lutein to β-CRX as well as metabolic engineering of microbial hosts for β-CRX recovery have been developed [7]. However, to our best knowledge, no natural β-CRX producer has been reported to date except for *K. marina* DAGII [1]. As a result, *K. marina* DAGII holds high significance in research and development due to its ability to naturally produce β-CRX as the final and major product [8].

One of the major obstacles of carotenoid production, however, is the use of overpriced substrates [9]. Thus, replacement with a low-cost substrate might significantly help in cost reduction. The dairy and cheese industry is an integral part of India's economy and, by far, India is one of the largest producers and consumers of milk and dairy products. However, during production of cheese and other products such as cottage cheese, 85–95% of the milk volume is removed as whey [10]. Whey is the liquid remnant produced during separation of coagulated casein and fat from milk [11]. It is considered that whey consists of 55% milk nutrients of which the majority includes lactose (4.5–5% w/v), soluble proteins (0.6–0.8% w/v), lipids (0.4–0.5% w/v), mineral salts (8–10% of dried extract), lactic (0.05% w/v) and citric acids, non-protein nitrogen compounds (urea and uric acid) and B group vitamins [12]. Production of 1 kg of cheese results in the generation of approximately 9 kg of whey which is mostly disposed of unutilized [13]. It is roughly estimated that India accounts for an annual whey production of 2 million tonnes [14]. Thus, disposal of this huge quantity of whey is an environmental concern due to its high biological oxygen demand $(30–50\,g\,l^{-1})$ and chemical oxygen demand $(60–80\,g\,l^{-1})$ [15]. Mostly, whey is dumped into sewers or disposed of on land, which leads to detrimental impacts on health and the environment [16]. On the other hand, disposal into water bodies causes serious threat to aquatic life [10]. Thus, utilization of this whey for value addition could be a possible solution from health and environmental aspects. Cheese whey being a rich source of lactose could serve as an inexpensive fermentation medium for many microorganisms. To date, cheese whey has been used in different biotechnological processes for obtaining value added products such as ethanol, lactic acid, enzymes, biopolymers, biogas and single-cell protein [16]. In this context, our previous study on β-CRX production by *K. marina* DAGII using dual substrates has been extended by substituting the carbon sources with cheese whey for improved β-CRX production by *K. marina* DAGII [1].

Media design, optimization and kinetic modelling are crucial steps in a bioprocess. An effective production of the desired product requires development of a proper fermentation medium. Statistical approaches (response surface methodology (RSM) and artificial neural network (ANN)) are the ideal ways for media design and optimization of multivariable systems compared with the conventional 'one-factor-at-a-time' method which is not only tedious and time-consuming but also complicated for quantifying interactive effects of different factors in the process concerned [17]. In addition, analysis of rate equations for microbial growth, substrate uptake and product formation facilitates prediction of the behaviour of the biological system under different experimental conditions [18]. Thus establishment of mathematical models is also an indispensible step for commercial production of bioproducts.

In this present study, utilization of cheese whey as a substrate for β-CRX production was studied. The optimum medium composition for improved β-CRX production was validated using two statistical modelling approaches, RSM and ANN. Different unstructured kinetic models were developed to correlate between microbial growth, substrate concentration and product formation. The novelty of the research work lies in the utilization of a low-cost dairy residue, that is mostly disposed of as waste, for enhanced production of β-CRX. β-CRX production using cheese whey with optimization using ANN and validation with a kinetic model has not been reported so far.

2. Material and methods

2.1. Chemicals

All the media ingredients, i.e. brain heart infusion agar, yeast extract, peptone, glucose, maltose, sodium chloride, were purchased from Himedia, India. Solvents like methanol, petroleum benzene were HPLC grade and purchased from Merck, India. Reagents for lactose estimation, i.e. zinc acetate, phosphotungstic acid, glycine, sodium hydroxide, methylamine, sodium sulfite and lactose monohydrate, were purchased from Himedia, India. Standard β-CRX was obtained from Sigma-Aldrich, USA.

2.2. Microorganism, growth medium and inoculum preparation

Kocuria marina DAGII (accession number: KF498648) was isolated from soil in the Department of Biotechnology, NIT Durgapur, West Bengal, India [2]. The bacterium was maintained on a growth medium consisting of glucose ($7.5\,\mathrm{g\,l^{-1}}$), maltose ($10.0\,\mathrm{g\,l^{-1}}$), yeast extract ($10.0\,\mathrm{g\,l^{-1}}$), peptone ($5.0\,\mathrm{g\,l^{-1}}$) and sodium chloride ($4.0\,\mathrm{g\,l^{-1}}$) with an initial pH of 7.9 [1]. Inoculum preparation was done as described by Mitra *et al.* [19]; 1% (v/v) of the inoculum with an optical density of 0.4–0.6 was used in all experiments.

2.3. Cheese whey preparation

Cheese whey was obtained from a local dairy shop (Durgapur, West Bengal, India). The precipitates were removed by centrifugation at 3220*g* for 10 min. The clear liquid was collected for further use.

2.4. Cultivation medium and culture conditions

Cheese whey was added to the growth medium and the concentration of the constituents was varied according to the experimental design. The Erlenmeyer flasks were incubated in a rotary shaker (150 r.p.m.) at 25°C for 120 h.

2.5. Dry weight, lactose measurement and carotenoid estimation

Biomass concentration was measured by the dry weight method and expressed in $\mathrm{g\,l^{-1}}$ [20]. The lactose content was determined by following the method of Nickerson *et al*. [21]. Briefly, cheese whey samples were reacted with methylamine in hot alkaline solution and the resulting red coloured solution was spectrophotometrically measured at 540 nm. The lactose content in the samples was determined from the standard curve of lactose and expressed in $\mathrm{g\,l^{-1}}$. β-CRX was extracted by a two-stage solvent extraction method as described by Mitra *et al*. [1]. Concentration of the extracted β-CRX was determined from the standard curve prepared using standard β-CRX and expressed as $\mathrm{mg\,l^{-1}}$ of culture.

2.6. Application of response surface methodology to optimize β-cryptoxanthin and biomass production by *Kocuria marina* DAGII

2.6.1. Design of experiments

DESIGN-EXPERT software (v. 8.0.7.1, Stat-Ease, Minneapolis, USA) was used for optimization of β-CRX and biomass production by *K. marina* DAGII. Optimization of the β-CRX and biomass production was done by central composite design (CCD). Four independent variables, namely yeast extract (A), peptone (B), cheese whey (C) and initial pH (D), were evaluated and coded to +1, 0 and −1 levels which corresponded to high, medium and low values, respectively (electronic supplementary material, table S1). In addition, the axial points were coded as +2 and −2 (electronic supplementary material, table S1). The four variables and their respective ranges were chosen based on the literature and preliminary experimental study. The β-CRX yield and biomass were modelled as the responses.

2.7. Artificial neural networks modelling

Artificial neural networks (ANNs) are powerful learning systems that are based on the principles of the human nervous system [22]. ANN is also known as neural nets, artificial neural system, parallel

distributed processing system and connectionist system [23]. During the past few decades, ANN has emerged as an attractive tool for nonlinear multivariate modelling. In this study, a three-layer feed-forward network with sigmoid hidden neurons and linear output neurons was used to build an ANN model where the four variables (i.e. yeast extract, peptone, cheese whey and pH) served as input and the β-CRX yield and biomass were output. Since the data distribution in CCD experimental design is statistically uniform in the input domain, it is effectively used in ANN [24]. However for better accuracy, a higher number dataset is suggested, and thus 200 data points were additionally developed using the quadratic equation for β-CRX yield and biomass (electronic supplementary material, equations S1 and S2) [25]. In total, 230 data points were fed to the ANN architecture. The Levenberg–Marquardt back-propagation algorithm was employed for training the network. The ANN modelling was executed using MATLAB R2014a (v. 8.3, MathWorks®, USA).

2.8. Kinetic modelling

In this study, unstructured mathematical models for kinetic analysis were developed by taking into consideration the following assumptions:

(1) There was no oxygen limitation in the culture.
(2) There was no limitation by nitrogen.

2.8.1. Microbial growth

A logistic kinetic model was used to simulate the growth of *K. marina* DAGII under varying cheese whey concentrations. Logistic equations are sets of equations that characterize growth in terms of maximum attainable biomass concentration, which is identical to the ecological concept of carrying capacity [26]. It is an independent model that can adequately describe the growth inhibition, a phenomenon that frequently occurs in batch culture [27]. The logistic model can be represented by equation (2.1), where μ is the specific growth rate (h^{-1}), X is the biomass concentration ($g\,l^{-1}$), X_m is the maximum biomass concentration ($g\,l^{-1}$) that can be obtained from a particular fermentation system (corresponding to the carrying capacity) and $(1 - (X/X_m))$ represents the unused carrying capacity [26].

$$\frac{dX}{dt} = \mu X \left(1 - \frac{X}{X_m}\right). \tag{2.1}$$

Integration of the above equation using boundary condition as $X(0) = X_0$ results in a sigmoidal curve representing both the exponential and stationary phases by the variation of X as a function of time, t.

$$X = \frac{X_0 e^{\mu t}}{1 - (X_0/X_m)(1 - e^{\mu t})}. \tag{2.2}$$

2.8.2. Lactose consumption kinetics

Cheese whey was used as the substrate for growth and β-CRX production by *K. marina* DAGII. The lactose content in cheese whey was determined spectrophotometrically using the method of Nickerson *et al.* [21]. Further, the lactose utilization was modelled by logistic mass balance equation, which can be represented by equation (2.3), where S_L is lactose concentration ($g\,l^{-1}$), Y_{X/S_L} ($g_{cell\ biomass}\ g_{lactose}{}^{-1}$) is the maximum yield coefficient and m_C ($g_{lactose}\ g_{cell\ biomass}{}^{-1}\ h^{-1}$) is the maintenance coefficient [28].

$$-\frac{dS_L}{dt} = \frac{1}{Y_{X/S_L}}\frac{dX}{dt} + m_C X. \tag{2.3}$$

Integration of the equation (2.3) using boundary condition as $S_L(0) = S_{L0}$ at $t = 0$ results in equation (2.4), where S_{L0} is the initial lactose concentration.

$$-[S_L - S_{L0}] = \frac{1}{Y_{X/S_L}}[X]_0^t + m_C \int_0^t X \, dt. \tag{2.4}$$

Taking into consideration the equation for X (equation (2.2)), equation (2.4) can be represented as:

$$-[S_L - S_{L0}] = \frac{1}{Y_{X/S_L}}\left[\frac{X_0 X_m e^{\mu t}}{X_m - X_0 + X_0 e^{\mu t}} - \frac{X_0 X_m e^0}{X_m - X_0 + X_0 e^0}\right] + m_C \int_0^t \frac{X_0 X_m e^{\mu t}}{X_m - X_0 + X_0 e^{\mu t}} dt. \tag{2.5}$$

To solve the integral part, temperature T was defined as an exponential function of μt [28] which can further be differentiated to

$$dT = \mu e^{\mu t} dt. \tag{2.6}$$

Hence, the equation (2.5) can be finally written as:

$$S_L = S_{L0} - \frac{X_0 X_m e^{\mu t}}{Y_{X/S_L}(X_m - X_0 + X_0 e^{\mu t})} + \frac{X_0}{Y_{X/S_L}} - \frac{X_m m_C}{\mu} \ln \frac{X_m - X_0 + X_0 e^{\mu t}}{X_m}. \tag{2.7}$$

The values of Y_{X/S_L} and m_C were estimated from the nonlinear regression of S_L and t.

2.8.3. Product formation kinetics

The β-CRX production by *K. marina* DAGII was described using the Leudeking–Piret kinetics equation [29]. According to this equation, the rate of product formation is directly and linearly proportional to growth rate and instantaneous biomass concentration and can be mathematically represented as:

$$\frac{dP}{dt} = \alpha \frac{dX}{dt} + \beta X, \tag{2.8}$$

where α is the growth associated product formation coefficient (exponential phase) and β is the non-growth associated product formation coefficient (stationary phase). The integrated form can be represented as:

$$\int_0^P dP = \alpha \int_{0-\Delta t}^{t-\Delta t} \frac{dX}{dt} dt + \beta \int_{0-\Delta t}^{t-\Delta t} X dt. \tag{2.9}$$

The term 'Δt' was introduced to describe the delay in β-CRX production with respect to cell growth [28]. By substituting equation (2.2), equation (2.10) was generated which represents the nonlinear relationship between the product (P) and time (t).

$$P = \alpha \left(\frac{X_0 X_m e^{\mu(t-\Delta t)}}{X_m - X_0 + X_0 e^{\mu(t-\Delta t)}} - \frac{X_0 X_m e^{-\mu \Delta t}}{X_m - X_0 + X_0 e^{-\mu \Delta t}} \right)$$
$$+ \frac{X_m \beta}{\mu} \left[\ln \left(\frac{X_m - X_0 + X_0 e^{\mu(t-\Delta t)}}{X_m} \right) - \ln \left(\frac{X_m - X_0 + X_0 e^{-\mu \Delta t}}{X_m} \right) \right]. \tag{2.10}$$

2.9. Statistical analysis

All experiments were conducted in triplicate and results were reported as their averaged values. GraphPad PRISM® v. 6.07 (GraphPad Software, Inc., USA) was employed in order to estimate the kinetic parameters from the model equations. The method of least squares was used to minimize the sum of the squares of the vertical distances between the points and the curve during regression analysis. The sum of the squares (SS) was calculated by equation (2.11), where y_i and f_i are the predicted data and experimental data, respectively, and n represents the length of the actual data period.

$$SS = \sum_{i=1}^{n} (y_i - f_i)^2. \tag{2.11}$$

The goodness of estimation was expressed by correlation coefficient R^2, variance (σ), standard deviation of residuals ($S_{y.x}$) and mean squared error (MSE). R^2 and variance (σ) were determined using MS EXCEL. $S_{y.x}$ (expressed in the same units as y-axis) was calculated from the sum of squares (SS) and degrees of freedom (d.f., equal to number of data points minus the number of parameters fit) as:

$$S_{y.x} = \sqrt{\frac{SS}{d.f.}}. \tag{2.12}$$

The MSE value was calculated by dividing the sum of squares by length of actual data period as:

$$MSE(\%) = \left(\frac{SS}{n} \right) \times 100. \tag{2.13}$$

3. Results and discussion

3.1. Screening of significant factors

The growth medium was supplemented with cheese whey and the effect of each medium component on β-CRX production was studied by deleting one or more factors. A set of 33 experiments with different medium composition was designed. Fourfold increase in β-CRX production ($p < 0.05$) was observed when glucose and maltose were substituted with cheese whey. Thus, yeast extract, peptone and cheese whey were selected as the significant contributing factors for CCD design. Additionally, pH was considered because it is an important parameter determining the growth of microbes.

The optimization of the factors responsible for β-CRX and biomass production by *K. marina* DAGII was performed.

3.1.1. Experimental results and analysis of variance

To examine the relationship between the responses and the four independent factors, a series of experiments were performed. The number of experiment required for the development of CCD was defined as:

$$N = 2^n + 2n + n_C. \tag{3.1}$$

where N is the total number of experiments, n is the number of factors and n_C is the number of central points [30]. With four factors, CCD consists of 16 factorial design runs, eight axial runs and six central points. The series of experiments and the corresponding values for the responses are shown in table 1. A multiple regression analysis was performed using DESIGN-EXPERT and a quadratic model was suggested for the best fit model of β-CRX ($R^2 = 0.9888$, $R_{Adj}^2 = 0.9783$, $R_{Pre}^2 = 0.9590$, Adeq. precision = 34.403) and biomass production ($R^2 = 0.9820$, $R_{Adj}^2 = 0.9801$, $R_{Pre}^2 = 0.9606$, Adeq. precision = 37.344). Higher R^2 values and Adeq. precision greater than 4 indicate high adequacy of a model. Thus, in our case, the values justified the model fitting. The results were analysed using analysis of variance (ANOVA) (table 2). The model F-values, p-values and lack of fit were used as a tool to evaluate the significance of the models. The F-value of 129.0 and 343.77 for β-CRX and biomass production, respectively, implied the model was significant. Model p-values (Prob > F) were significant (<0.0001) whereas the lack of fit was found to be insignificant (p-value$_{β-CRX}$ = 0.8213, p-value$_{biomass}$ = 0.2032). To understand the interacting effects, the p-values were further used to check the significance of the coefficients. A Pareto chart was designed to understand the contribution of each factor (figure 1). In the Pareto chart, effects have been standardized and arranged in the order of significance. The lengths of the bars are proportional to the magnitude of the estimated coefficients of the effects. The vertical line represents the minimum magnitude of the statistically significant effects of the response with a 95% CI. The coefficient estimates and the corresponding p-values suggested that individual factors were significant ($p < 0.05$) but yeast extract (A) had the largest effect, followed by cheese whey (figure 1). in the case of β-CRX production, the significance of peptone was more than that of pH. The interactive effect of yeast extract–peptone (AB) was found to be highest, followed by yeast extract–cheese whey (AC) and peptone–cheese whey (BC). The other interactive effects were found to be insignificant. All the quadratic terms (A^2, B^2, C^2 and D^2) were found to be significant ($p < 0.0001$). The final model equation in terms of coded factors is given below:

$$β\text{-CRX yield}(mg\,l^{-1}) = 16.09 + 2.17A + 1.27B + 1.34C + 0.37D - 0.98AB$$

$$- 0.81AC - 0.18AD - 0.67BC - 0.14BD + (1.184 \times 10^{-003})CD$$

$$- 1.84A^2 - 0.84B^2 - 0.92C^2 - 1.53D^2, \tag{3.2}$$

where positive terms signified synergistic effect and negative terms signified antagonistic effect [31]. The contour diagram along with 3D response surface diagrams of the significant interactions are shown in figure. 2. Figure 2*a* shows the effect of yeast extract and peptone and their correlation between each other. When yeast extract and peptone concentrations were kept at minimum levels (i.e. 5 and 2.5 g l^{-1}, respectively), the β-CRX yield was approximately 9 mg l^{-1}. The β-CRX yield increased to 15 mg l^{-1} when the yeast extract concentration increased at fixed peptone concentration of 2.5 g l^{-1}. However, when the peptone concentration was increased by keeping yeast extract fixed at 5 g l^{-1}, β-CRX concentration increased to 13 mg l^{-1}. This showed that the contribution of yeast extract was more compared with peptone for β-CRX production and, thus, justified the variation in

Table 1. CCD design matrix of independent variables and their corresponding values of responses.

run	factor 1 A: yeast extract (g l^{-1})	factor 2 B: peptone (g l^{-1})	factor 3 C: cheese whey (% v/v)	factor 4 D: initial pH (unit)	response 1 β-CRX yield (mg l^{-1})	response 2 biomass (g l^{-1})
1	10	10	10	7.75	14.8140	3.82
2	10	5	10	7.75	17.0450	5.16
3	15	7.5	15	7	13.0575	3.69
4	15	7.5	5	7	14.0800	3.75
5	15	2.5	15	8.5	13.9652	4.07
6	5	2.5	5	8.5	04.2459	2.67
7	5	2.5	5	7	03.3500	2.43
8	10	5	10	7.75	16.7555	5.31
9	5	7.5	15	8.5	12.8590	4.15
10	20	5	10	7.75	13.0005	3.67
11	15	7.5	5	8.5	13.2780	3.23
12	5	2.5	15	7	08.6440	2.92
13	5	7.5	15	7	12.4416	3.66
14	15	2.5	5	7	11.0203	4.07
15	10	5	10	7.75	15.5215	5.21
16	10	0	10	7.75	10.2377	3.88
17	10	5	0	7.75	09.4441	3.45
18	10	5	10	9.25	10.6607	3.46
19	5	7.5	5	7	09.1972	3.15
20	10	5	10	7.75	15.9500	5.14
21	5	2.5	15	8.5	10.2473	3.92
22	10	5	10	7.75	15.6593	5.12
23	5	7.5	5	8.5	10.4346	3.17
24	0	5	10	7.75	04.1105	2.64
25	10	5	10	6.25	08.8854	3.05
26	15	2.5	5	8.5	12.4019	3.64
27	15	7.5	15	8.5	13.8017	3.90
28	10	5	20	7.75	15.0266	4.25
29	10	5	10	7.75	15.6155	5.12
30	15	2.5	15	7	13.9983	3.95

F-value. Probably the levels of amino acids and small peptides present in yeast extract were higher and they were easily transported and used by the cell for metabolite production [32]. Figure 2*b* shows an approximate increase in β-CRX yield from 9 to 13 mg l^{-1} when cheese whey concentration was increased keeping yeast extract concentration fixed at 5 g l^{-1}. When both the factors were kept at their maximum levels, the β-CRX yield was almost 16 mg l^{-1}. In figure 2*c*, it was observed that at a cheese whey concentration of 15% (v/v), the β-CRX yield increased from approximately 15 to 16.2 mg l^{-1} when peptone was varied from 2.5 to 7.5 g l^{-1}. Even at low concentration of cheese whey (i.e. 5% v/v) and peptone (2.5 g l^{-1}), the β-CRX yield was considerably higher (approx. 11 mg l^{-1}). This suggested that the nutritional components of cheese whey enhanced the β-CRX production by *K. marina* DAGII.

Table 2. Analysis of variance for the quadratic model for β-CRX and biomass.

| source	sum of squares	degrees of freedom	mean square	*F*-value	$p > F$
β-CRX yield					
model	379.5	14	27.11	94.32	<0.0001
A-yeast extract	112.51	1	112.51	391.48	<0.0001
B-peptone	38.58	1	38.58	134.24	<0.0001
C-cheese whey	43.13	1	43.13	150.06	<0.0001
D-pH	3.37	1	3.37	11.73	0.0038
AB	15.24	1	15.24	53.02	<0.0001
AC	10.44	1	10.44	36.31	<0.0001
AD	0.51	1	0.51	1.78	0.2017
BC	7.11	1	7.11	24.74	0.0002
BD	0.32	1	0.32	1.1	0.3105
CD	2.24×10^{-5}	1	2.24×10^{-5}	7.81×10^{-5}	0.9931
A^2	92.39	1	92.39	321.48	<0.0001
B^2	19.48	1	19.48	67.78	<0.0001
C^2	22.98	1	22.98	79.97	<0.0001
D^2	64.29	1	64.29	223.69	<0.0001
residual	4.31	15	0.287393		
lack of fit	2.2	10	0.220255	0.52	0.8213
pure error	2.11	5	0.421671		
cor total	383.81	29			
biomass					
model	18.98	14	1.355677	133.56	<0.0001
A-yeast extract	1.65	1	1.651913	162.75	<0.0001
B-peptone	0.034	1	0.033863	3.34	0.0477
C-cheese whey	1.36	1	1.363982	134.38	<0.0001
D-pH	0.16	1	0.158681	15.63	0.0013
AB	0.7	1	0.697851	68.75	<0.0001
AC	0.33	1	0.33394	32.9	<0.0001
AD	0.35	1	0.351501	34.63	<0.0001
BC	6.20×10^{-5}	1	6.2×10^{-5}	6.1×10^{-3}	0.9387
BD	0.033	1	0.03317	3.27	0.0907
CD	0.4	1	0.397373	39.15	<0.0001
A^2	7.02	1	7.015331	691.17	<0.0001
B^2	3.04	1	3.043525	299.86	<0.0001
C^2	3.03	1	3.032115	298.73	<0.0001
D^2	6.37	1	6.368598	627.45	<0.0001
residual	0.15	15	0.01015		
lack of fit	0.12	10	0.012373	2.17	0.2032
pure error	0.029	5	0.005704		
cor total	19.13	29			
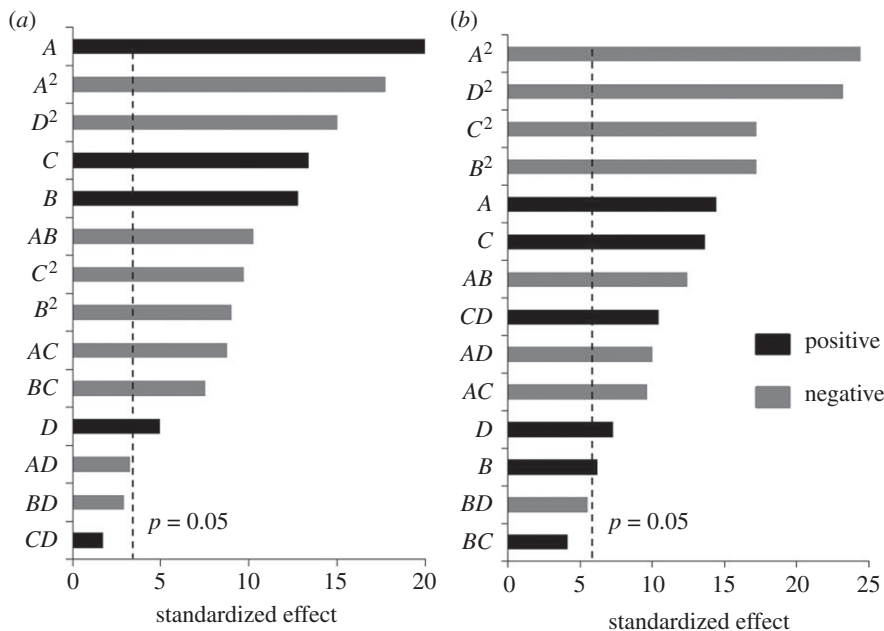
Figure 1. Standardized Pareto chart for β-CRX (*a*) and biomass (*b*).

In the case of biomass production, the interactive effects of yeast extract–peptone (*AB*), yeast extract–cheese whey (*AC*), yeast extract–pH (*AD*) and cheese whey–pH (*CD*) were found to be significant (figure 1). Similar to β-CRX production, all the quadratic terms were significant. The final equation for regression was found to be

$$
\begin{aligned}
\text{biomass} = {}& 5.18 + 0.26A + 0.038B + 0.24C + 0.081D \\
& - 0.21AB - 0.14AC - 0.15AD + (1.969 \times 10^{-003})BC - 0.046BD \\
& + 0.16CD - 0.51A^2 - 0.33B^2 - 0.33C^2 - 0.48D^2.
\end{aligned}
\tag{3.3}
$$

Figure 3 shows the contour plots and the corresponding 3D diagrams for biomass production. Figure 3*a* shows an increase in biomass yield from 3.76 to 4.7 g l^{-1} when the yeast extract was varied from 5.0 to 15 g l^{-1} at constant peptone concentration of 2.5 g l^{-1}. Figure 3*b* depicted the relationship between yeast extract and cheese whey and it was clearly evident that biomass production gradually increased with cheese whey concentration. Figure 3*c*,*d* shows the relationship of yeast extract and cheese whey with pH, respectively. Both the figures suggested that variation of pH increased the biomass; however, above pH 7.75 the biomass reduced. Probably alkaline pH slowed the bacterial growth [33].

The electronic supplementary material, figure S1 shows the correlation between the experimental and predicted values of β-CRX and biomass yield obtained from the model, respectively. Distribution of the data points shows adequate agreement between the experimental and predicted values. This proved that the predicted quadratic model was appropriate to navigate the design space defined by the CCD. CCD has long been used as an important statistical tool for optimization. For instance in 2007, cell growth and carotenoid biosynthesis in *Xanthophyllomyces dendrorhous* was successfully optimized using CCD. Similarly, Imamoglu *et al.* [34] statistically evaluated the physical growth parameters of *Dunaliella salina* strain EgeMacc-024 during batch production of chlorophyll *a*. In 2015, hydrolysis of cassava fibrous waste (a hugely produced solid waste during processing of cassava tubers in sago industries in India) to obtain maximum glucose yield was done using CCD and a quadratic polynomial equation predicting the optimal points was developed [35]. In another study, CCD was employed for enhanced co-production of xylanase and lichenase by *Bacillus subtilis* D3d using different agro-industrial residues [36].

3.1.2. Optimization and verification study

The optimum values of the four variables for β-CRX and biomass production were obtained by numerical optimization using DESIGN-EXPERT 8.0.7.1. β-CRX yield and biomass were maximized by
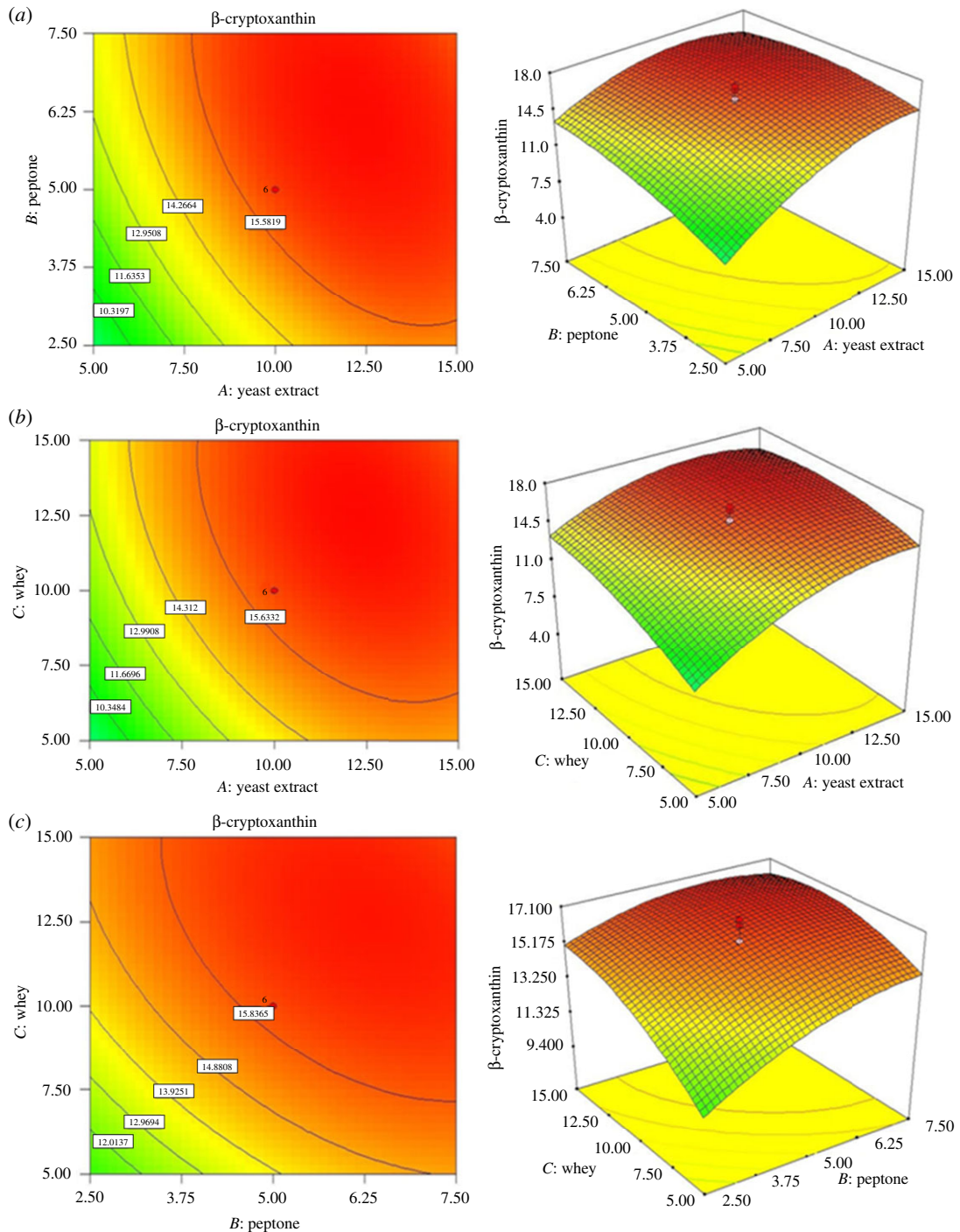
Figure 2. Contour plots and their corresponding 3D diagrams for β-CRX yield.

keeping the four independent factors 'in range'. The maximum production was obtained at $11.47\,\mathrm{g\,l^{-1}}$ yeast extract, $5.29\,\mathrm{g\,l^{-1}}$ peptone, 12.00% (v/v) cheese whey and pH 7.83. The predicted values of β-CRX ($16.95\,\mathrm{mg\,l^{-1}}$) and biomass ($5.23\,\mathrm{g\,l^{-1}}$) yield were further verified by conducting three additional experiments at the obtained optimum condition. The average experimental values were found to be $17.14\,\mathrm{mg\,l^{-1}}$ and $5.35\,\mathrm{g\,l^{-1}}$, respectively, which were in good agreement with the predicted values and, thus, validated the model obtained by CCD. In a similar study by Khodaiyan *et al*. [37], maximum canthaxanthin yield of $2.871\pm0.076\,\mathrm{mg\,l^{-1}}$ was obtained at whey lactose concentration of $55.54\,\mathrm{g\,l^{-1}}$, yeast extract concentration of $7.36\,\mathrm{g\,l^{-1}}$ and pH of 7.66.
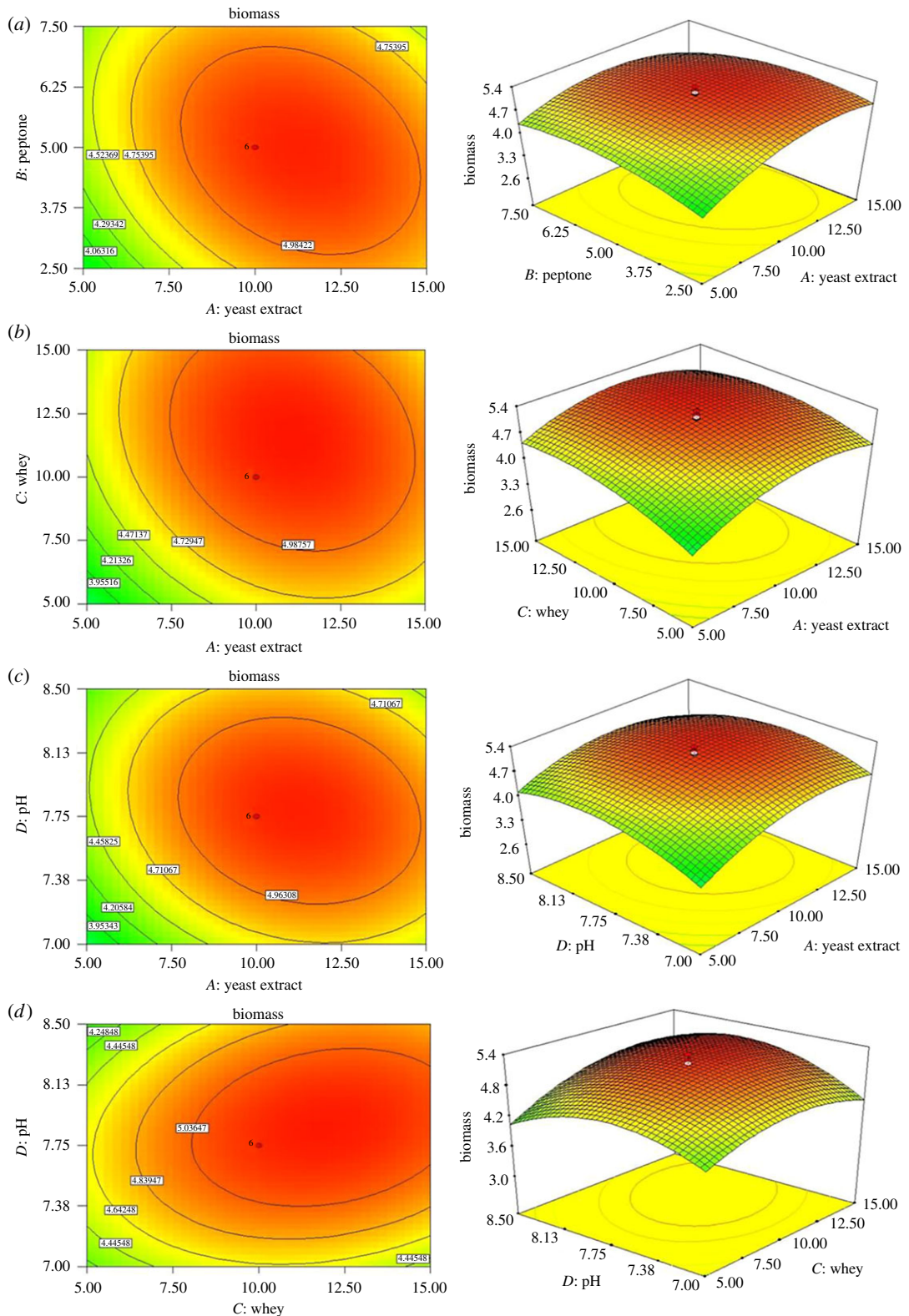
Figure 3. Contour plots and their corresponding 3D diagrams for biomass.

3.2. Prediction of responses with artificial neural network

The electronic supplementary material, figure S2 shows the ANN model constructed with input layer, hidden layer and output layer. The input layer consisted of four neurons, i.e. concentrations of yeast extract, peptone, cheese whey and pH. The output layer consisted of
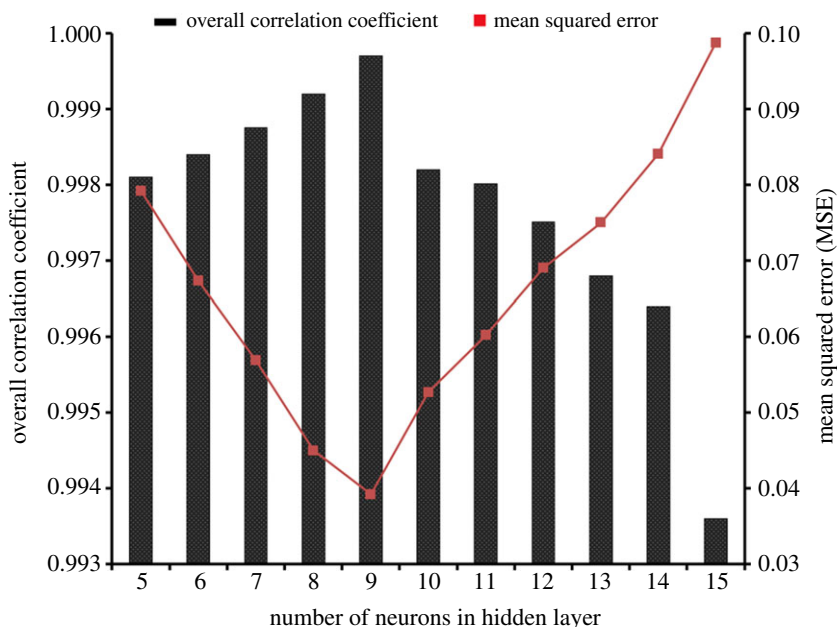
Figure 4. Effect of neuron number on ANN model.

two neurons, i.e. β-CRX yield and biomass. In a feed-forward back-propagation algorithm, input information is transmitted to the output layer through neurons of a hidden layer. To determine the number of neurons in the hidden layer, MSE and R^2 of different neural networks were evaluated on a trial and error basis (figure 4). A network consisting of a hidden layer with nine neurons gave the best result. The ANN model was trained with 160 samples, validated with 35 samples and the accuracy of the model and prediction were further tested with 35 samples.

The Levenberg–Marquardt algorithm used in the present study is a standard iterative technique that localizes local minimum of a multivariate function by expressing sum of squares of several nonlinear, real-valued functions in a short time [38]. Using this algorithm training automatically stops when generalization stops improving, which is indicated by an increase in the MSE of the validation samples. From the electronic supplementary material, figure S3, it was observed that best validation was achieved at epoch 7. The correlations between the experimental and the predicted results are given in figure 5. As indicated by the R^2 values, ANN served as a reliable prediction model in our study. Moreover, the MSE for the entire dataset was significantly low, as depicted by the error histogram (electronic supplementary material, figure S4), which suggested that the ANN model possessed good approximation characteristics. The ANN predicted yield of β-CRX and biomass was found to be 16.99 mg l^{-1} and 5.33 g l^{-1}, respectively. It was evident from the values of R^2 and predicted yield that even though both the models (RSM as well as ANN) fitted well to the experimental design, ANN offered better predictive and approximation accuracy. The better predictive accuracy of ANN can be attributed to the fact that it can universally approximate the nonlinearity of any system and additionally it has the ability to calculate multiple responses in a single run. By contrast, RSM can be implemented only upto second-order polynomial and it must be run multiple times for multiple responses (run number equal to number of responses to be predicted) [39]. In 2014, Rafigh *et al*. [40] successfully modelled the curdlan production from *Paenibacillus polymyxa* using RSM and ANN and suggested that ANN reported more stable responses. In a study by Azad *et al*. [41], the ANN model showed distinct superiority compared with the RSM model during optimization of process parameters for adsorption of ternary dyes by nickel doped ferric oxyhydroxide FeO(OH) nanowires on activated carbon. Recently, a feed-forward back-propagation algorithm was effectively implemented to develop an ANN model for improved ε-polylysine production by the marine bacterium *B. licheniformis* [25].

From this entire work, it was found that substitution of the previous carbon source (i.e. glucose and maltose) with the help of cheese whey gave fourfold increase in β-CRX production and 1.7-fold increase in biomass. Finally, validation of RSM statistical data with the help of the ANN method resulted into 4.67- and 2.34-fold increase in β-CRX yield and biomass, respectively. Probably
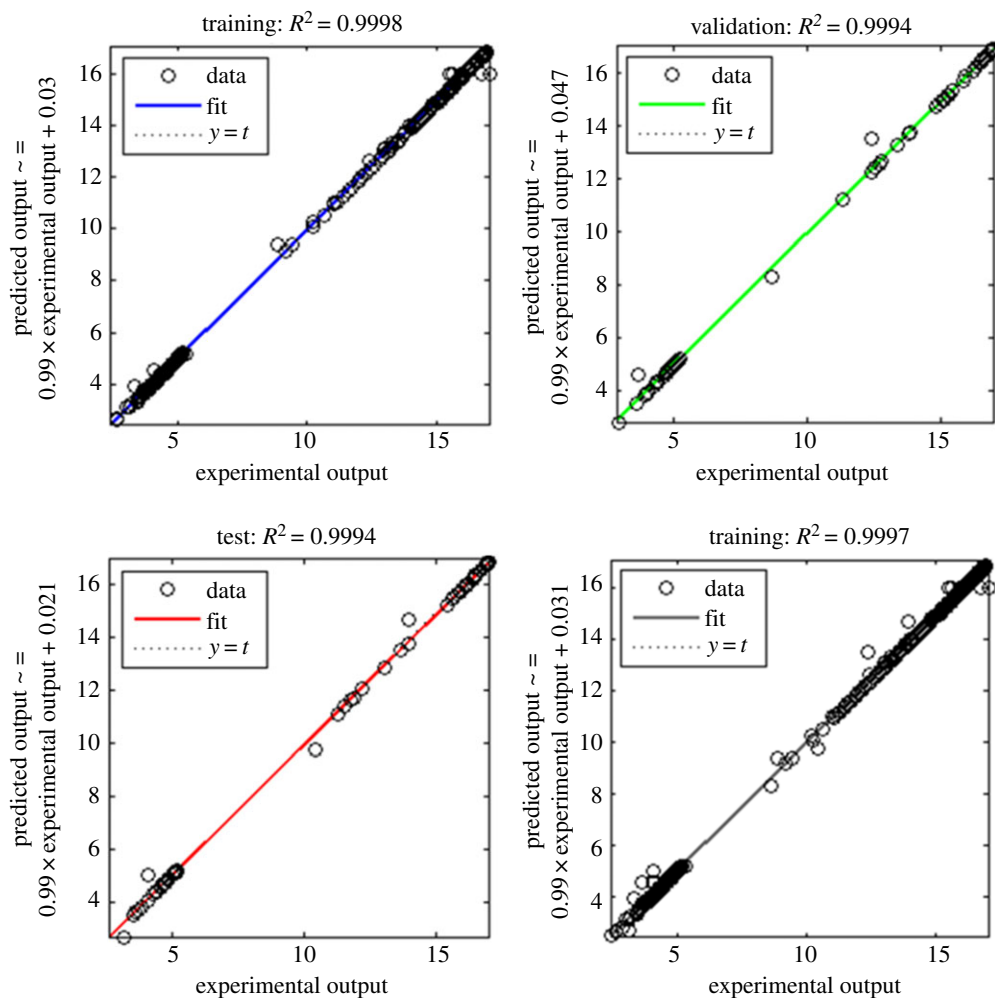
Figure 5. Experimental result versus ANN predicted output.

cheese whey utilization increases the acetyl-CoA pool in the bacterium which eventually increases the production of isopentenyl pyrophosphate (IPP) and dimethylallyl diphosphate (DMADP) through the mevalonic acid pathway. As IPP and DMADP are the key precursors of carotenogenesis, an increased concentration of both the precursors is leading to increased β-CRX production by *K. marina* DAGII.

3.3. Kinetic modelling of *Kocuria marina* DAGII

Kinetic modelling helps in accessing the interaction between microbial growth and the surrounding environment. It helps in predicting the behaviour of microbial processes under different environmental conditions. Most importantly, the quantitative knowledge of kinetic parameters helps in analysis, optimization, design and operation of biological processes at large scale conditions [42]. Thus, development of a mathematical model is an important step for better understanding of microbial kinetics. Structured mathematical models involve intracellular metabolism of the biosystem, which makes the process complicated. On the other hand, unstructured models consider only biomass as its principal variable which makes its implementation simple and robust [43].

3.3.1. Microbial growth kinetics

Kocuria marina DAGII showed a classical growth trend in the presence of cheese whey as substrate. Irrespective of the cheese whey concentration, the *K. marina* DAGII cells entered the exponential phase after a lag phase of 4 h. During lag phase, the physiologically active bacterial cells adapted to the new experimental environment but no apparent growth was observed. Once the acclimatized cells entered the
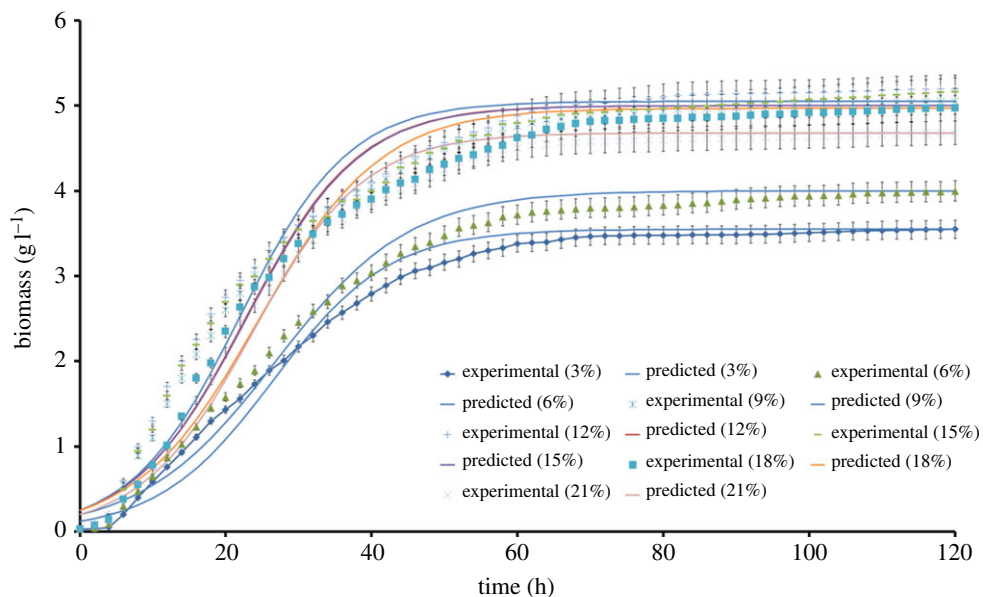
Figure 6. Fitting of the experimental data to the logistic model describing cell growth over time at 3.0–21.0% (v/v) of initial cheese whey concentration.

exponential phase the biomass increased at a constant rate; however, the growth slowed down during its transition to stationary phase at 38–48 h. In our previous study, it was observed that in the presence of glucose and maltose as carbon source, *K. marina* DAGII achieved stationary phase at 25 h [1]. However, substitution of the carbon source with cheese whey delayed the onset of nutrient depletion by 24 h and, thus, the exponential phase continued for a longer time period. A logistic equation was employed to describe the growth kinetics of the *K. marina* DAGII and it was observed that the simulated growth profile was in good agreement with the experimental growth curve for all the cheese whey concentrations, as indicated in figure 6. The kinetic parameters were obtained by fitting the experimental data into the logistic equations (table 3). The low values of statistical parameters such as sum of squares (SS), standard deviation of residuals ($S_{y.x}$) and MSE signified the good fit of the model. Additionally, the high R^2 values (>0.90) suggested that the logistic model successfully described the sigmoidal growth pattern of the bacterium taking into consideration the growth inhibition that took place in the stationary phase. According to a number of researchers, logistic equations have been successful in predicting sigmoidal growth patterns of different bacteria under a batch mode of operations [44]. However, it was noteworthy that the specific growth rate (μ) and maximum biomass yield (X_m) of *K. marina* DAGII increased when the cheese whey concentration was increased from 3 to 12% (v/v), but after 12% (v/v) a gradual decrease was noted (table 3). This indicated that above 12% (v/v), cheese whey played an inhibitory role during the growth of *K. marina* DAGII and thus necessitated the implementation of a substrate inhibition model for estimation of inhibition parameters. Cell growth during batch production of lutein by heterotrophic *Chlorella* decreased as the glucose concentration was increased from 10 to 60 g l^{-1} [45]. Similarly, carotenoid production by *X. dendrorhous* using *Yucca fillifera* date juice as substrate was studied by Luna-Flores *et al.* [46], and it was found that cell growth decreased when substrate concentration was increased from 20 to 40 g l^{-1}. In 2016, Kim *et al.* [47] reported that specific growth rate of *Klebsiella oxytoca* during 2,3-butanediol production increased with increase in glucose concentration up to 32 g l^{-1} and thereafter gradually decreased.

3.3.2. Substrate consumption

Substrate utilization is an important factor governing cell growth and β-CRX production. The lactose utilization results were incorporated into the logistic mass balance equation and the kinetic parameters were calculated as shown in table 3. The S_0, Y_{X/S_L} and m_C at the varying cheese whey concentrations were calculated. The values of R^2, SS, $Sy.x$, MSE% depicted that the fitting results were satisfactory (table 3). Moreover, the graphical representation of the experimental and predicted lactose consumption clearly justified the fitness of the experimental data into the logistic mass balance model (figure 7). The

Table 3. Kinetic parameter for growth at different cheese whey concentrations.

parameter estimation	cheese whey concentration (% v/v)						
microbial growth	3	6	9	12	15	18	21
X_0 (g l^{-1})	0.0300	0.0320	0.0290	0.0310	0.0350	0.0330	0.0260
X_m (g l^{-1})	3.5500	4.0000	5.0500	5.2000	5.1700	4.9700	4.6800
μ (h^{-1})	0.0421	0.0837	0.1243	0.1518	0.1427	0.1260	0.1074
R^2	0.9805	0.9827	0.9733	0.9681	0.9595	0.9715	0.9859
σ	1.4351	1.7424	2.5258	2.5442	2.5215	2.5854	2.3475
SS	1.801	1.599	1.968	2.043	2.1631	1.983	1.472
$S_{y.x}$ (g l^{-1})	0.1718	0.1619	0.1796	0.1830	0.1883	0.1803	0.1553
MSE (%)	2.9524	2.6213	3.2262	3.3491	3.5460	3.2508	2.4131
lactose consumption							
S_{L0} (g l^{-1})	3.5	3.91	4.06	4.22	4.36	4.58	4.76
m_C (g$_{lactose}$ g$_{biomass}$$^{-1}$ h^{-1})	0.0027	0.0029	0.0031	0.0034	0.0029	0.0029	0.0028
Y_{X/S_L} (g$_{biomass}$ g$_{lactose}$$^{-1}$)	12.28	13.22	14.82	16.95	14.9	13.31	12.25
R^2	0.9857	0.9832	0.9948	0.9989	0.9889	0.9809	0.9913
σ	0.2809	0.2975	0.2187	0.2032	0.2634	0.2991	0.2491
SS	0.0387	0.0486	0.0181	0.0046	0.0456	0.0847	0.0376
$S_{y.x}$ (g l^{-1})	0.0656	0.0735	0.0449	0.0226	0.0712	0.0970	0.0646
MSE (%)	0.3525	0.4420	0.1649	0.0420	0.4149	0.7705	0.3419
β-CRX production							
α (mg$_{\beta-CRX}$ g$_{biomass}$$^{-1}$)	1.029	1.294	1.598	1.958	1.607	1.548	1.498
β (mg$_{\beta-CRX}$ g$_{biomass}$$^{-1}$ h^{-1})	0.0150	0.0174	0.0198	0.0199	0.0199	0.0192	0.01813
Δt (h)	2.546	2.582	2.494	2.161	2.055	2.347	2.161
R^2	0.9991	0.9987	0.9998	0.9993	0.9989	0.9992	0.9992
σ	0.2230	0.2360	0.2085	0.2203	0.2263	0.2318	0.2338
SS	0.5919	0.6499	0.6018	0.6113	0.6284	0.646	0.5968
$S_{y.x}$ (mg l^{-1})	0.0739	0.0812	0.0752	0.0764	0.0785	0.0807	0.0746
MSE (%)	0.0538	0.0590	0.0547	0.0555	0.0571	0.0587	0.0542

values of Y_{X/S_L} exhibited an increasing trend when the cheese whey concentration was increased from 3 to 12% (v/v). After 12% (v/v), the Y_{X/S_L} decreased gradually. It could be inferred that after a certain concentration of lactose, the bacterium was unable to use the excess substrate. In a similar study by Goswami *et al.* [48], it was reported that the yield coefficient decreased when the glucose concentration was increased beyond $15\,\mathrm{g\,l^{-1}}$ during batch production of canthaxanthin by *Dietzia maris* NITD. The maintenance coefficient (m_C) varied slightly with cheese whey concentration. According to Shuler & Kargi [26], the maintenance coefficient (m_C) is the parameter that describes the specific rate of substrate uptake for cellular maintenance and can be represented as

$$m_C = \frac{\mathrm{d}S/\mathrm{d}t_{m_C}}{X}. \tag{3.4}$$

The maintenance coefficient is considered as a measure for substrate utilization for non-growth related activities such as energy required by the cell for repairing damaged cellular components, transferring nutrients and products in and out of the cell, for mobility and for adjusting osmolarity of the cell interior. Thus, it is likely that yield coefficient values will depend on the maintenance coefficient. Depending upon the environmental conditions of the cell, the values of m_C might vary from 0.02 to 4.0 g$_{lactose}$ g$_{biomass}$$^{-1}$ h^{-1} [49]. During the kinetic modelling study of hyaluronic acid production by
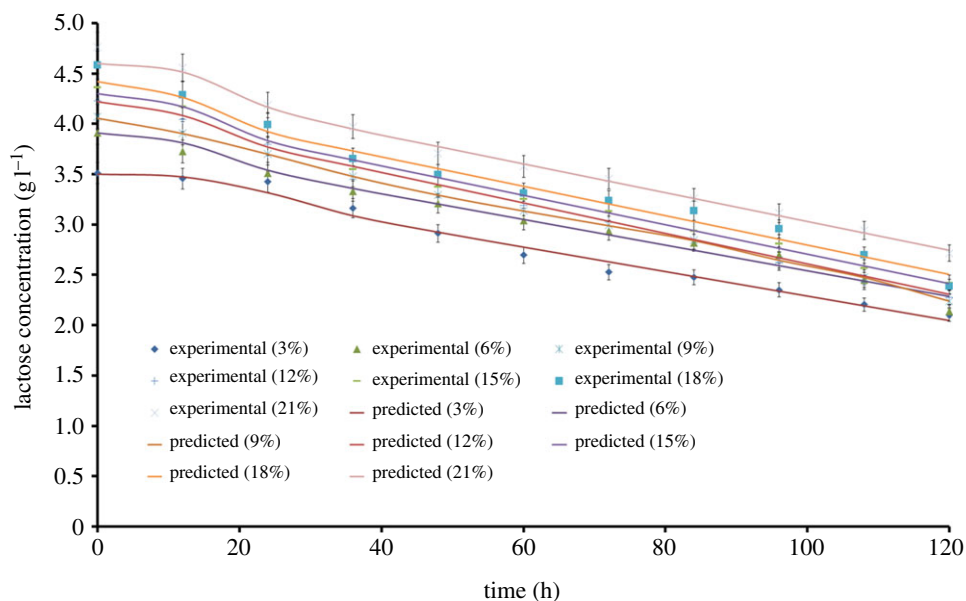
Figure 7. Fitting of the experimental data to the model describing lactose consumption with time at varying cheese whey concentrations.

Streptococcus zooepidemicus, 'm_C' ranged from 0.04 to 1.56 ($g_{glucose}$ $g_{cell\ biomass}^{-1}$ h^{-1}) with variation in glucose concentration [28]. The 'm_C' value was found to be 0.0699 $g\ g^{-1}\ d^{-1}$ during ajmalicine production from hairy roots of *Catharanthus roseus* using sucrose as the substrate [50]. Thus, the above discussion suggests that the logistic mass balance equations adequately describe the lactose consumption by *K. marina* DAGII during β-CRX production.

3.3.3. β-Cryptoxanthin production

During the fermentation, β-CRX production increased with time and the maximum concentration was obtained at 120 h of incubation. The corresponding β-CRX concentration at 3, 6, 9, 12, 15, 18 and 21% (v/v) of cheese whey was found to be 9.8, 13.5, 15.4, 17.14, 16.23, 15.84, 14.45 mg l^{-1}, respectively. The experimental data were fitted to the Luedeking–Piret model and the values of α, β and Δt were determined from the resulting nonlinear regression (table 3). The high R^2 values indicated that the experimental data fitted well into the model. The observation was further justified by the low values of SS, $Sy.x$ and MSE%. Moreover, the predicted data was in accordance with the experimental data as depicted in figure 8. The variation in α and β values suggested that the maximum yield was obtained at 12% (v/v) of cheese whey. Cheese whey concentrations beyond 12% (v/v) inhibited the β-CRX production (table 3). The decrease could be due to catabolic repression and reduced specific growth rate at higher concentrations of cheese whey [47]. During the fermentation process, the cells serve as the factory for metabolite production, probably; thus growth inhibition at higher substrate concentration results in the reduced product formation. The Δt was found to be in the range of 2.0–2.6 h which indicated that the pigment production was mostly growth dependent and also justified the higher magnitude of α compared to β. In the study by Don & Shoparwe [28], production kinetics showed that lag time between the hyaluronic acid production and cell growth of *S. zooepidemicus* varied from 0.49 to 2.16 h. The Luedeking–Piret model was also successfully implemented by Gutiérrez-Arnillas *et al*. [51] to elucidate the metabolic characteristics of lipolytic enzymes synthesized by halophilic microorganisms. The study further reported the product to be a secondary metabolite based on the values of α and β.

3.3.4. Model development for substrate inhibition

Based on the results of previous sections, it was observed that higher concentrations of cheese whey inhibited the cell growth of *K. marina* DAGII. It was even plausible that higher product concentration was responsible for the decreased cell growth. However, in the present study, the specific growth rate remained fairly constant with respect to time during the exponential phase of the bacterial growth which indicated that the inhibition occurred due to the substrate.
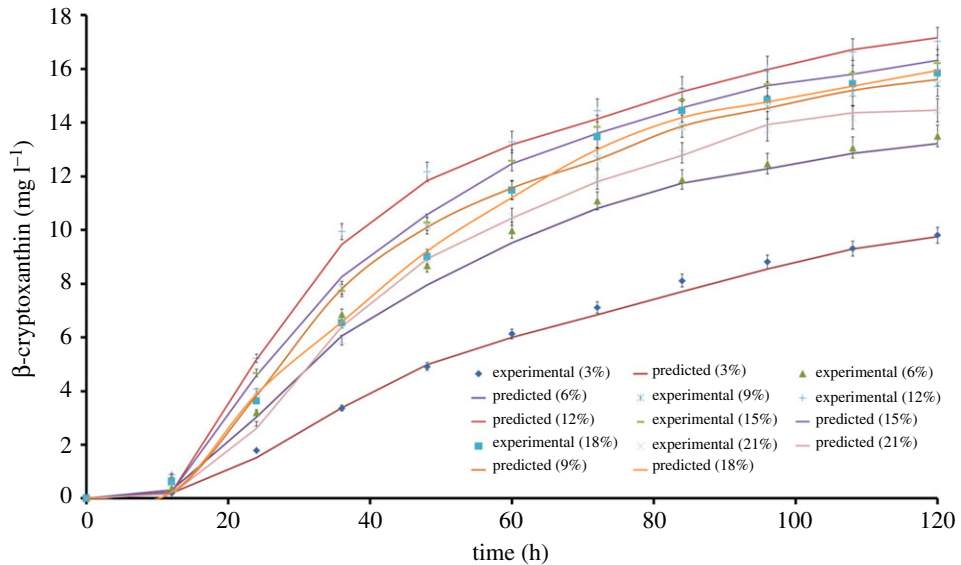
Figure 8. Fitting of the experimental data to the Luedeking–Piret model describing β-CRX production over time at 3.0–21.0% (v/v) of initial cheese whey concentrations.
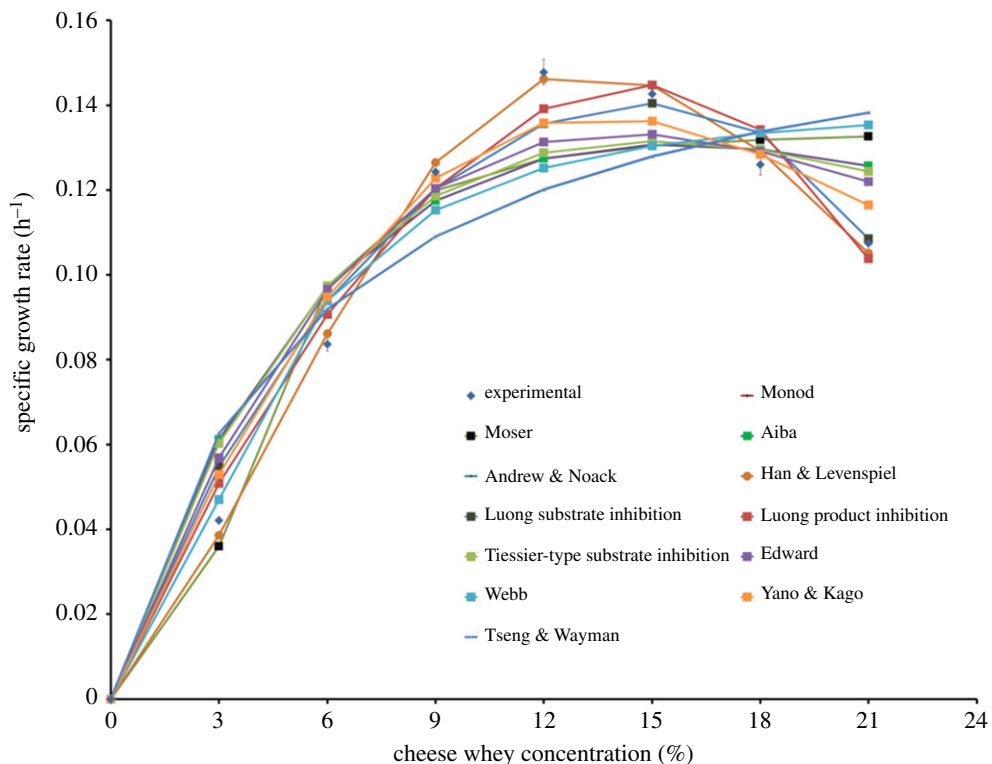

Figure 9. Comparison of the experimental data and model simulations at different initial cheese whey concentrations.

When the μ values (obtained from the logistic model) were fitted to the Monod model, it failed to validate the experimental data. Thus, other unstructured kinetic models were used and the data were validated (electronic supplementary material, table S2). The μ values at all the varying cheese whey concentrations were fitted to the models and the biokinetic parameters such as μ_{max} (maximum specific growth rate), K_s (Monod half saturation constant), K_i (substrate inhibition concentration), S_m (maximum substrate inhibition constant above which cells cease to grow), and K_1, K_2, n and m (constants correlating between μ and substrate) were evaluated and the results shown in the electronic supplementary material,

table S3. The graphical representation of the simulated and the experimental data is shown in figure 9. The fitness of the models was quantified by evaluating R^2, σ, SS, $Sy.x$ and MSE%. Based on these statistical analyses, it was observed that the highest R^2 value and lowest σ, SS, $Sy.x$ and MSE% values were obtained in the case of the Han and Levenspiel model. The Han and Levenspiel model is a generalized form of Monod kinetics which is based on the assumption that there exists a critical substrate concentration above which cells cease to grow, and the constants of the Monod equation are functions of this limiting inhibitor concentration [52]. The model equation describing the cell growth with cheese whey as substrate can be represented as given in equation (3.5), where S is the initial cheese whey concentration:

$$\mu = 0.2385\left(1 - \frac{S}{27.40}\right)^{0.5576}\left(\frac{S}{S + 22.06(1 - (S/27.40))^{3.868}}\right). \tag{3.5}$$

4. Conclusion

Optimization and kinetic modelling of a fermentation process have been successfully described in the present study. The statistical tools RSM and ANN were used for elucidating the optimal condition for β-CRX production by *K. marina* DAGII using cheese whey as the substrate. Significantly high β-CRX yield was achieved when carbon sources were substituted with 12% (v/v) cheese whey. The results suggested that both RSM and ANN showed stable predictive responses but ANN was more accurate for data fitting and estimation capabilities. The kinetic models for cell growth, substrate consumption and product formation were analysed. Logistic equations adequately described the growth profile of *K. marina* DAGII under varying cheese whey concentrations and the substrate consumption was well defined by logistic mass balance equation. The product formation coefficients were evaluated using the Luedeking–Piret model with high accuracy. With reference to the substrate inhibition, the Han and Levenspiel model fitted best with the experimental data. In our opinion, utilization of cheese whey for production of valuable products such as carotenoids is an optimistic approach for value addition and a cleaner environment.

References

1. Mitra R, Chaudhuri S, Dutta D. 2017 Modelling the growth kinetics of *Kocuria marina* DAGII as a function of single and binary substrate during batch production of β-cryptoxanthin. *Bioprocess Biosyst. Eng.* **40**, 99–113. (doi:10.1007/s00449-016-1678-6)

2. Mitra R, Samanta AK, Chaudhuri S, Dutta D. 2017 Effect of selected physico-chemical factors on bacterial β-cryptoxanthin degradation: stability and kinetic study. *J. Food Process Eng.* **40**, e12379. (doi:10.1111/jfpe.12379)

3. Cilla A, Attanzio A, Barberá R, Tesoriere L, Livrea MA. 2015 Anti-proliferative effect of main dietary phytosterols and β-cryptoxanthin alone or combined in human colon cancer Caco-2 cells through cytosolic Ca^{+2}- and oxidative stress-induced apoptosis. *J. Funct. Foods* **12**, 282–293. (doi:10.1016/j.jff.2014.12.001)

4. Sahin K, Orhan C, Akdemir F, Tuzcu M, Sahin N, Yilmaz I, Juturu V. 2017 β-Cryptoxanthin ameliorates metabolic risk factors by regulating NF-κB and Nrf2 pathways in insulin resistance induced by high-fat diet in rodents. *Food Chem. Toxicol.* **107**, 270–279. (doi:10.1016/j.fct.2017.07.008)

5. Pongkan W *et al.* 2017 Beta-cryptoxanthin exerts better cardioprotection against cardiac ischemia-reperfusion injury than astaxanthin via protecting mitochondrial dysfunction in mice. *J. Am. Coll. Cardiol.* **69**, 104. (doi:10.1016/S0735-1097(17)33493-9)

6. Yamaguchi M. 2012 Role of carotenoid β-cryptoxanthin in bone homeostasis. *J. Biomed. Sci.* **19**, 36–48. (doi:10.1186/1423-0127-19-36)

7. Sunilkumar TKD, Shankaranarayana ML, Sherena PA, Shankaranaarayanan J. 2015 US Patent no. 20150361040 A1.

8. Samanta AK, Chaudhuri S, Dutta D. 2016 Antioxidant efficacy of carotenoid extract from bacterial strain *Kocuria marina* DAGII. *Mater. Today Proc.* **3**, 3427–3433. (doi:10.1016/j.matpr.2016.10.023)

9. Cheng YT, Yang CF. 2016 Using strain *Rhodotorula mucilaginosa* to produce carotenoids using food wastes. *J. Taiwan Inst. Chem. Eng.* **61**, 270–275. (doi:10.1016/j.jtice.2015.12.027)

10. Bansal S, Oberoi HS, Dhillon GS, Patil RT. 2008 Production of β-galactosidase by *Kluyveromyces marxianus* MTCC 1388 using whey and effect of four different methods of enzyme extraction on β-galactosidase activity. *Ind. J. Microbiol.* **48**, 337–341. (doi:10.1007/s12088-008-0019-0)

11. Das M, Raychaudhuri A, Ghosh SK. 2016 Supply chain of bioethanol production from whey: a review. *Proc. Environ. Sci.* **35**, 833–846. (doi:10.1016/j.proenv.2016.07.100)

12. Amado IR, Vázquez JA, Pastrana L, Teixeira JA. 2016 Cheese whey: a cost-effective alternative for hyaluronic acid production by *Streptococcus zooepidemicus*. *Food Chem.* **198**, 54–61. (doi:10.1016/j.foodchem.2015.11.062)

13. Karthika C, Sharmila G, Muthukumaran C, Manikandan K. 2013 Utilization of whey powder as an alternate carbon source for production of hypocholesterolemic drug by *Aspergillus terreus* MTCC 1281. *Food Sci. Biotechnol.* **22**, 1–7. (doi:10.1007/s10068-013-0220-8)

14. Patowary R, Patowary K, Kalita MC, Deka S. 2016 Utilization of paneer whey waste for cost-effective production of rhamnolipid biosurfactant. *Appl. Biochem. Biotechnol.* **180**, 383–399. (doi:10.1007/s12010-016-2105-9)

15. Das B, Sarkar S, Sarkar A, Bhattacharjee S, Bhattacharjee C. 2016 Recovery of whey proteins and lactose from dairy waste: a step towards green waste management. *Process Saf. Environ. Prot.* **101**, 27–33. (doi:10.1016/j.psep.2015.05.006)

16. Yadav JS, Bezawada J, Elharche S, Yan S, Tyagi RD, Surampalli RY. 2014 Simultaneous single-cell protein production and COD removal with characterization of residual protein and intermediate metabolites during whey fermentation by *K. marxianus*. *Bioprocess Biosyst. Eng.* **37**, 1017–1029. (doi:10.1007/s00449-013-1072-6)

17. Talib NA, Salam F, Yusof NA, Ahmad SA, Sulaiman Y. 2017 Optimization of peak current of poly(3,4-ethylenedioxythiophene)/multi-walled carbon nanotube using response surface methodology/central composite design. *RSC Adv.* **7**, 11 101–11 110. (doi:10.1039/C6RA26135C)

18. Gharibzahedi SM, Razavi SH, Mousavi M. 2013 Kinetic analysis and mathematical modeling of cell growth and canthaxanthin biosynthesis by *Dietzia natronolimnaea* HS-1 on waste molasses hydrolysate. *RSC Adv.* **3**, 23 495–23 502. (doi:10.1039/C3RA44663H)

19. Mitra R, Samanta AK, Chaudhuri S, Dutta D. 2015 Growth kinetics and carotenoid production of a newly isolated bacterium on glucose as a carbon source during batch fermentation. In *Int. Conf. on Advances in Biotechnology (BioTech) Proceedings*. Singapore: Global Science and Technology Forum.

20. Mitra R, Samanta AK, Chaudhuri S, Dutta D. 2016 Impact of carbon source on β-cryptoxanthin production by *Kocuria marina* DAGII: a classical approach. *Mater. Today Proc.* **3**, 3269–3275. (doi:10.1016/j.matpr.2016.10.008)

21. Nickerson TA, Vujicic IF, Lin AY. 1976 Colorimetric estimation of lactose and its hydrolytic products. *J. Dairy Sci.* **59**, 386–390. (doi:10.3168/jds.S0022-0302(76)84217-8)

22. Kavitha B, Thambavani DS. 2016 Kinetics, equilibrium isotherm and neural network modeling studies for the sorption of hexavalent chromium from aqueous solution by quartz/feldspar/wollastonite. *RSC Adv.* **6**, 5837–5847. (doi:10.1039/C5RA22851D)

23. Markopoulos AP, Manolakos DE, Vaxevanidis NM. 2008 Artificial neural network models for the prediction of surface roughness in electrical discharge machining. *J. Intell. Manuf.* **19**, 283–292. (doi:10.1007/s10845-008-0081-9)

24. Desai KM, Survase SA, Saudagar PS, Lele SS, Singhal RS. 2008 Comparison of artificial neural network (ANN) and response surface methodology (RSM) in fermentation media optimization: case study of fermentative production of scleroglucan. *Biochem. Eng. J.* **41**, 266–273. (doi:10.1016/j.bej.2008.05.009)

25. Bhattacharya S, Dineshkumar R, Dhanarajan G, Sen R, Mishra S. 2017 Improvement of ϵ-polylysine production by marine bacterium *Bacillus licheniformis* using artificial neural network modeling and particle swarm optimization technique. *Biochem. Eng. J.* **126**, 8–15. (doi:10.1016/j.bej.2017.06.020)

26. Shuler ML, Kargi F. 2002 *Bioprocess engineering: basic concepts*, 2nd edn. Englewood Cliffs, NJ: Prentice-Hall.

27. Liu JZ, Weng LP, Zhang QL, Xu H, Ji LN. 2003 A mathematical model for gluconic acid fermentation by *Aspergillus niger*. *Biochem. Eng. J.* **14**, 137–141. (doi:10.1016/S1369-703X(02)00169-9)

28. Don MM, Shoparwe NF. 2010 Kinetics of hyaluronic acid production by *Streptococcus zooepidemicus* considering the effect of glucose. *Biochem. Eng. J.* **49**, 95–103. (doi:10.1016/j.bej.2009.12.001)

29. Luedeking R, Piret EL. 1959 A kinetic study of the lactic acid fermentation. Batch process at controlled pH. *J. Biochem. Microbiol. Technol. Eng.* **1**, 393–412. (doi:10.1002/jbmte.390010406)

30. Bera S, Sharma VP, Dutta S, Dutta D. 2016 Biological decolorization and detoxification of malachite green from aqueous solution by *Dietzia maris* NIT-D. *J. Taiwan Inst. Chem. Eng.* **67**, 271–284. (doi:10.1016/j.jtice.2016.07.028)

31. Ab Ghani Z, Yusoff MS, Zaman NQ, Zamri MF, Andas J. 2017 Optimization of preparation conditions for activated carbon from banana pseudo-stem using response surface methodology on removal of color and COD from landfill leachate. *Waste Manage.* **62**, 177–187. (doi:10.1016/j.wasman.2017.02.026)

32. Klotz S, Kuenz A, Prüße U. 2017 Nutritional requirements and the impact of yeast extract on the D-lactic acid production by *Sporolactobacillus inulinus*. *Green Chem.* **19**, 4633–4641. (doi:10.1039/C7GC01796K)

33. Wang J, Jonkers HM, Boon N, De Belie N. 2017 *Bacillus sphaericus* LMG 22257 is physiologically suitable for self-healing concrete. *Appl. Microbiol. Biotechnol.* **101**, 5101–5114. (doi:10.1007/s00253-017-8260-2)

34. Imamoglu E, Demirel Z, Dalay MC. 2014 Evaluation of culture conditions of locally isolated *Dunaliella salina* strain EgeMacc-024. *Biochem. Eng. J.* **92**, 22–27. (doi:10.1016/j.bej.2014.05.008)

35. Cingadi S, Srikanth K, Arun EV, Sivaprakasam S. 2015 Statistical optimization of cassava fibrous waste hydrolysis by response surface methodology and use of hydrolysate based media for the production of optically pure D-lactic acid. *Biochem. Eng. J.* **102**, 82–90. (doi:10.1016/j.bej.2015.02.006)

36. Moteshafi H, Mousavi SM, Hashemi M. 2016 Enhancement of xylanase productivity using industrial by-products under solid suspended fermentation in a stirred tank bioreactor, with a dissolved oxygen constant control strategy. *RSC Adv.* **6**, 35 559–35 567. (doi:10.1039/C6RA01449F)

37. Khodaiyan F, Razavi SH, Mousavi SM. 2008 Optimization of canthaxanthin production by *Dietzia natronolimnaea* HS-1 from cheese whey using statistical experimental methods. *Biochem. Eng. J.* **40**, 415–422. (doi:10.1016/j.bej.2008.01.016)

38. Sapna S, Tamilarasi A, Kumar MP. 2012 Backpropagation learning algorithm based on Levenberg Marquardt Algorithm. *Comp. Sci. Inform. Technol.* **2**, 393–398. (doi:10.5121/csit.2012.2438)

39. Youssefi S, Emam-Djomeh Z, Mousavi SM. 2009 Comparison of artificial neural network (ANN) and response surface methodology (RSM) in the prediction of quality parameters of spray-dried pomegranate juice. *Drying Technol.* **27**, 910–917. (doi:10.1080/07373930902988247)

40. Rafigh SM, Yazdi AV, Vossoughi M, Safekordi AA, Ardjmand M. 2014 Optimization of culture medium and modeling of curdlan production from *Paenibacillus polymyxa* by RSM and ANN. *Int. J. Biol. Macromol.* **70**, 463–473. (doi:10.1016/j.ijbiomac.2014.07.034)

41. Azad FN, Ghaedi M, Asfaram A, Jamshidi A, Hassani G, Goudarzi A, Azqhandi MH, Ghaedi A. 2016 Optimization of the process parameters for the adsorption of ternary dyes by Ni doped FeO(OH)-NWs–AC using response surface methodology and an artificial neural network. *RSC Adv.* **6**, 19 768–19 779. (doi:10.1039/C5RA26036A)

42. Bera S, Dutta D. 2017 Encapsulation and release of a bacterial carotenoid from hydrogel matrix: characterization, kinetics and antioxidant study. *Eng. Life Sci.* **17**, 739–748. (doi:10.1002/elsc.201600238)

43. Benkortbi O, Hanini S, Bentahar F. 2007 Batch kinetics and modelling of pleuromutilin production by *Pleurotus mutilis*. *Biochem. Eng. J.* **36**, 14–18. (doi:10.1016/j.bej.2006.06.015)

44. Chang HX, Huang Y, Fu Q, Liao Q, Zhu X. 2016 Kinetic characteristics and modeling of microalgae *Chlorella vulgaris* growth and CO_2 biofixation considering the coupled effects of light intensity and dissolved inorganic carbon. *Bioresour. Technol.* **206**, 231–238. (doi:10.1016/j.biortech.2016.01.087)

45. Wu ZY, Shi CL, Shi XM. 2007 Modeling of lutein production by heterotrophic *Chlorella* in batch and fed-batch cultures. *World J. Microbiol. Biotechnol.* **23**, 1233–1238. (doi:10.1007/s11274-007-9354-2)

46. Luna-Flores CH, Ramírez-Cordova JJ, Pelayo-Ortiz C, Femat R, Herrera-López EJ. 2010 Batch and fed-batch modeling of carotenoids production by *Xanthophyllomyces dendrorhous* using *Yucca fillifera* date juice as substrate. *Biochem. Eng. J.* **53**, 131–136. (doi:10.1016/j.bej.2010.10.004)

47. Kim DK, Park JM, Song H, Chang YK. 2016 Kinetic modeling of substrate and product inhibition for 2,3-butanediol production by *Klebsiella oxytoca*. *Biochem. Eng. J.* **114**, 94–100. (doi:10.1016/j.bej.2016.06.021)

48. Goswami G, Chakraborty S, Chaudhuri S, Dutta D. 2012 Optimization of process parameters by response surface methodology and kinetic modeling for batch production of canthaxanthin by *Dietzia maris* NIT-D (accession number: HM151403). *Bioprocess Biosyst. Eng.* **35**, 1375–1388. (doi:10.1007/s00449-012-0726-0)

49. Sinclair CG, Kristiansen B, Bu'Lock JD. 1987 *Fermentation kinetics and modeling*. Milton Keynes: Open University Press.

50. Thakore D, Srivastava AK, Sinha AK. 2015 Model based fed batch cultivation and elicitation for the overproduction of ajmalicine from hairy roots of *Catharanthus roseus*. *Biochem. Eng. J.* **97**, 73–80. (doi:10.1016/j.bej.2015.02.005)

51. Gutiérrez-Arnillas E, Rodriguez A, Sanroman MA, Deive FJ. 2016 New sources of halophilic lipases: isolation of bacteria from Spanish and Turkish saltworks. *Biochem. Eng. J.* **109**, 170–177. (doi:10.1016/j.bej.2016.01.015)

52. Han K, Levenspiel O. 1988 Extended Monod kinetics for substrate, product and cell inhibition. *Biotechnol. Bioeng.* **32**, 430–447. (doi:10.1002/bit.260320404)

53. Mitra R, Dutta D. 2018 Data from: Growth profiling, kinetics and substrate utilization of low-cost dairy waste for production of β-cryptoxanthin by *Kocuria marina* DAGII. Dryad Digital Repository. (http://dx.doi.org/10.5061/dryad.jd8bh)